

# Stochastic model of breakdown nucleation under intense electric fields - Supplemental Material

Eliyahu Zvi Engelberg, Yinon Ashkenazy, and Michael Assaf  
*Racah Institute of Physics and the Center for Nanoscience and Nanotechnology,  
 Hebrew University of Jerusalem, Jerusalem 9190401, Israel*  
 (Dated: March 22, 2018)

## CREATION AND DEPLETION RATES

In this section we describe the considerations leading to the formulation of the kinetic equations, leading up to Eq. (1) in the main text.

The rate at which new mobile dislocations are created in a slip plane is determined by the density of sources, which is proportional to the density of in-plane pre-existing defects  $c$  and the mobile dislocation density  $\rho$ . Both of these quantities represent in-plane densities, and therefore are measured in units of  $1/\text{nm}$ . Based on the amount of defects we see in experimental samples, we assign  $c$  a value of  $1 \mu\text{m}^{-1}$ .

In addition, the rate is proportional to the rate of creation of dislocations by each defect. Since the creation of dislocations is thermally activated, the rate should be inversely proportional to a temperature-dependent factor  $\exp[(E_a - \Omega\sigma)/(k_B T)]$ , divided by the creation time of each dislocation. Here  $E_a$  and  $\Omega$  are the activation energy and volume, respectively, of a dislocation nucleation source, whose values we estimate in the main text, while  $\sigma$  is the surface stress of the metal.

To find the attempt frequency of the nucleation, we consider, for convenience, a Frank-Read type source. The creation time of a dislocation in such a source is  $t = L/v$ , with  $L$  the length of the source, and  $v$  the velocity of the dislocation. The threshold stress needed to activate a source of length  $L$  or longer is  $\sigma_{th} = 2Gb/L$ , where  $G = 48 \text{ GPa}$  is the shear modulus, and  $b = 0.25 \text{ nm}$  is the Burgers vector [1]. If the amount of sources decreases rapidly as a function of length, then  $L \approx 2Gb/\sigma$ . For stresses ranging from  $0.2$  [2, 3] up to  $400 \text{ MPa}$  [4, 5], the dislocation velocity in Cu is approximately a linear function of  $\sigma$ ,  $v = 50C_t\sigma/G$ , where  $C_t = 2.31 \times 10^3 \text{ m/s}$  is the propagation velocity of sound in Cu [4]. Therefore  $t = G^2b/(25C_t\sigma^2)$ , giving us a total creation rate

$$\dot{\rho}^+ = \frac{25\kappa C_t}{G^2b}(\rho + c)\sigma^2 e^{-\frac{E_a - \Omega\sigma}{k_B T}}, \quad (1)$$

where  $\kappa$  is a kinetic factor, combining the fraction of mobile dislocations that have been pinned and therefore contribute nucleation sources, and the activation entropy of the sources [6]. We estimate the value of  $\kappa$  in the main text.

Mobile dislocations can be depleted by interactions with other mobile dislocations as well as with pre-existing defects, and ejection to the surface. Assuming that the

last mechanism is considerably slower than the first two, we can write the depletion rate as  $\dot{\rho}^- = \xi\rho v(c + \rho)$ . Here  $\xi$  is a dimensionless proportionality factor, representing trap efficiency. For simplicity, we assign it a value of 1. Substituting once again for  $v$  we have

$$\dot{\rho}^- = \frac{50\xi C_t}{G}\sigma\rho(c + \rho). \quad (2)$$

The stress in metal subjected to an external electric field is composed of the Maxwell stress due to the external field  $E$  applied, and of the average internal stress created by the dislocations themselves. The Maxwell stress is  $\epsilon_0(\beta E)^2/2$ , with the dimensionless parameter  $\beta$  representing the ratio of the effective electric field at the mobile dislocation nucleation site to  $E$ .  $\beta$  is expected to depend both on surface geometry and the electric field distribution. Specifically,  $\beta$  is expected to vary with  $\rho$ , since it depends on the aspect ratio of protrusions created on the surface [7–9]. However, it can be shown by numerical analysis that in the regime of interest, as determined by the values of the rest of the parameters, the aspect ratio remains nearly constant until breakdown. Therefore, we consider it to be a constant over time, whose value we estimate in the main text, for every given cathode geometry.

The second term of the stress is proportional to  $Gb/d$ , where  $d$  is the average distance between dislocations [10, 11]. In the experimental setups examined in the main text, a pulsed electric field is applied, and the breakdown rate (BDR) is constant over time. Since there is no memory effect, we assume a constant sessile dislocation population whose contribution to the total stress from all slip planes saturates. As a result, we take into consideration only the stress caused by the mobile dislocations, whose density varies over time. In multi-slip plane systems  $d$  is proportional to  $\rho^{-1/2}$ , with  $\rho$  measured in units of  $\text{nm}^{-2}$  [10, 11]. However, when considering only one slip plane as in our model, we expect the relation to be  $d \sim \rho^{-1}$ , with  $\rho$  in units of  $\text{nm}^{-1}$ , as described above (and also see below). We therefore find that, altogether, the stress is  $\sigma = \epsilon_0(\beta E)^2/2 + ZGb\rho$ , where the dimensionless parameter  $Z$ , in the second term of the stress, is a structural parameter linking the stress to the dislocation density. For simplicity, we assign it a value of 1.

Defining new constants of the form  $\alpha \equiv \Omega/(k_B T)$ ,  $A_1 \equiv \epsilon_0(\beta E)^2/2$ ,  $a_2 \equiv ZGb$ ,  $B_1 \equiv 25\kappa C_t e^{-\frac{E_a}{k_B T}}/(G^2b)$ , and  $b_2 \equiv 50\xi C_t/G$ , we arrive at Eq. (1) in the main text.

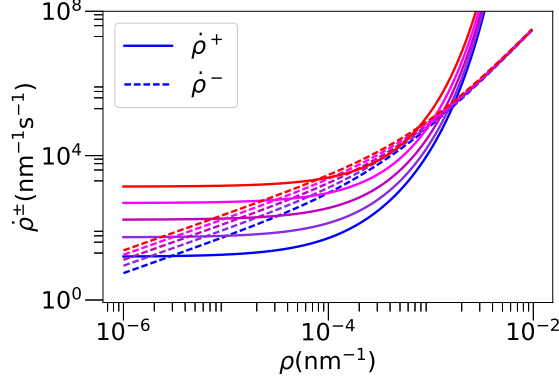


FIG. 1.  $\dot{\rho}^+$  and  $\dot{\rho}^-$  for five electric fields (bottom to top): 150, 190, 230, 270, and 310 MV/m.

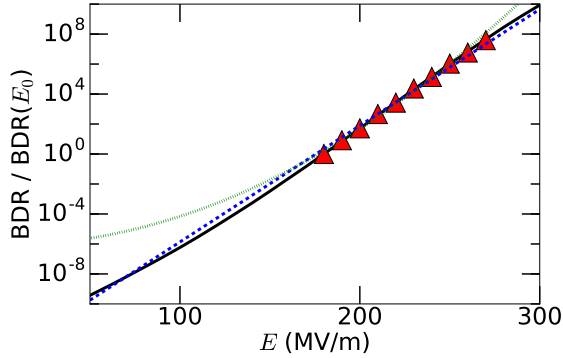


FIG. 2. BDR as a function of the electric field. The solid line is the metastable approximation [Eq. (9) in the main text], the triangles are the simulation results, and the dashed and dotted lines are linear and quadratic fits, respectively.

The values of  $\beta = 4.8 \pm 0.1$ ,  $\kappa = 0.41 \pm 0.02$ ,  $\Omega = 5.4 \pm 0.2$  eV/GPa, and  $E_a = 0.08 \pm 0.002$  eV, found by the fitting procedure in the main text, give us the following values for the constants:  $A_1 = 100 \text{ Pa (MV/m)}^{-2} E^2$ ,  $a_2 = 12 \text{ GPa nm}$ ,  $B_1 = 1850 \text{ MPa}^{-2} \text{ s}^{-1}$ ,  $b_2 = 2410 \text{ m GPa}^{-1} \text{ s}^{-1}$ ,  $c = 1 \text{ } \mu\text{m}^{-1}$ ,  $\alpha = 210 \text{ GPa}^{-1}$ . Figure 1 shows the values of  $\dot{\rho}^+$  and  $\dot{\rho}^-$  for the nominal values of the above parameters.

### LINEAR APPROXIMATION OF THE BDR

For practical purposes it is useful to identify a simple function of the dependence of the BDR on the electric field, which can be later fitted to experimental results. Our results strongly indicate that a linear fit of the logarithm serves as a good approximation over a wide range of electric fields, see Eq. (11) in the main text and Fig. 2 (for fields between 50 and 300 MV/m). Note that the pre-

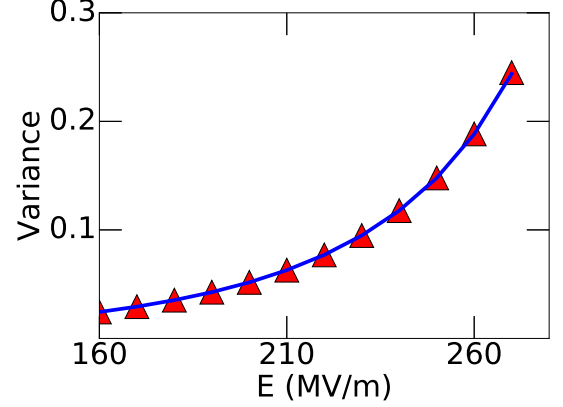


FIG. 3. Variance of the QSD as function of electric field: analytical result (lines), extracted from Eq. (7) in the main text, and simulation (triangles).

viously suggested dependence,  $\tau \sim \exp(\alpha E^2)$  [12], agrees with our model within the range of currently available data but significantly diverges from our results outside that range. However, we stress that our model includes a discernibly different temperature-dependent term, which can be distinguished by dedicated experiments.

### VARIANCE OF THE QSD

Figure 3 shows the variance of the quasi-stationary distribution (QSD) as a function of the electric field, for the same set of parameters as in Fig. 1. Here the simulation results agree well with a numerical calculation of the variance of the theoretical QSD [Eq. (7) in the main text]. As expected, for stronger fields the variance is larger, and the probability for breakdown increases, since the system moves more rapidly towards higher values of  $n$ . This increase in variance may be experimentally detected through increased variation in related signals such as the acoustic emission signal from moving dislocations within the electrodes, as well as in the dark current produced between them under increasing field.

### VOLUME DENSITY MODEL

The model developed in this manuscript discusses in-plane mobile dislocation density fluctuations, neglecting interactions between slip planes. The mobile dislocation density  $\rho$  is therefore a two-dimensional density, measured in units of length per area,  $\text{nm}^{-1}$ . If we were to define  $\rho$  as the volume density of mobile dislocations in units of length per volume,  $\text{nm}^{-2}$ , the average distance between dislocations would be proportional to  $\rho^{-1/2}$  [10, 11]. Then, the stress would be  $\sigma = \epsilon_0(\beta E)^2/2 + ZGb\rho^{1/2}$ . The

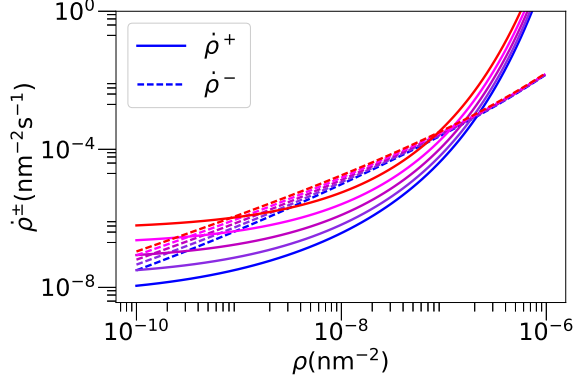


FIG. 4.  $\dot{\rho}^+$  and  $\dot{\rho}^-$  in a model describing volume mobile dislocation density fluctuations, for five electric fields (bottom to top): 150, 190, 230, 270, and 310 MV/m.

creation and depletion rates would be

$$\begin{aligned}\dot{\rho}^+ &= \frac{25\kappa C_t}{G^2 b} (\rho + c) \sigma^2 e^{-\frac{E_a - \Omega \sigma}{k_B T}} \\ \dot{\rho}^- &= \frac{50\xi C_t}{G} \sigma b \rho (c + \rho)\end{aligned}\quad (3)$$

where  $c = 1 \mu\text{m}^{-2}$  is now the volume density of the constant defects, while all other constants retain their original meaning. The factor of  $b$  in the depletion term was added in order to correctly describe the probability of two dislocations interacting, now in a volume instead of a plane, assuming that the width of a dislocation is equal

to the Burgers vector  $b$ .

As seen in Fig. 4, for adjusted values of the parameter set  $\beta$ ,  $\kappa$ ,  $\Omega$ , and  $E_a$ ,  $\dot{\rho}^+$  and  $\dot{\rho}^-$  as volume density creation and depletion rates exhibit the same qualitative behavior as in the two-dimensional density model. The same considerations as in the latter model can then be applied, once again yielding the  $\ln \tau \sim E$  dependence and BDRs as described in the main text.

- 
- [1] J. Weertman and J. R. Weertman, *Elementary Dislocation Theory* (MacMillan, New York, 1964).
  - [2] W. F. Greenman, T. Vreeland, Jr., and D. S. Wood, J. Appl. Phys. **38**, 3595 (1967).
  - [3] E. Nadgornyi, Prog. Mater. Sci. **31**, 1 (1988).
  - [4] J. P. Hirth and J. Lothe, *Theory of Dislocations* (Krieger, Malabar, FL, 1982).
  - [5] D. Mordehai, Y. Ashkenazy, I. Kelson, and G. Makov, Phys. Rev. B **67**, 024112 (2003).
  - [6] S. Ryu, K. Kang, and W. Cai, Proc. Natl. Acad. Sci. U.S.A. **108**, 5174 (2011).
  - [7] P. Chatterton, Proc. Phys. Soc. **88**, 231 (1966).
  - [8] X. Wang, M. Wang, P. He, Y. Xu, and Z. Li, J. Appl. Phys. **96**, 6752 (2004).
  - [9] A. Descoedres, Y. Levinsen, S. Calatroni, M. Taborelli, and W. Wuensch, Phys. Rev. Accel. Beams **12**, 092001 (2009).
  - [10] G. I. Taylor, Proc. R. Soc. A **145**, 362 (1934).
  - [11] J. Sevillano, P. van Houtte, and E. Aernoudt, Prog. Mater. Sci. **25**, 135 (1980).
  - [12] K. Nordlund and F. Djurabekova, Phys. Rev. Accel. Beams **15**, 071002 (2012).